Original article

The hazard rate function of the logistic Birnbaum-Saunders distribution: Behavior, associated inference, and application

Farouq Mohammad A. Alam [a,*], Abeer Mansour Almalki [a]

[a] *Department of Statistics, Faculty of Science, King Abdulaziz University, Jeddah 21589, Saudi Arabia*

A B S T R A C T

The hazard (failure) rate is a fundamental statistical indicator commonly used in both reliability and survival analyses. In practice, the hazard curve might exhibit a non-monotonic unimodal behavior. Thus, determining the highest point of the peak of a non-monotonic hazard function is indeed a point of interest in lifetime analysis. This study discusses the shape of the hazard function of the logistic Birnbaum-Saunders distribution and associate estimation. This model belongs to the generalized Birnbaum-Saunders family of positively skewed models with lighter and heavier tails than the conventional two-parameter Birnbaum-Saunders distribution. The latter model originated from a problem related to material fatigue, a phenomenon of interest in material sciences. In this paper, we establish that the hazard rate of the logistic Birnbaum-Saunders distribution is either unimodal or decreasing depending on the value of the shape parameter. We also estimate the critical value of the hazard rate, which is the highest point of the peak of the hazard function, using moment estimators. We perform extensive Monte Carlo simulations to examine estimation efficiency numerically; moreover, we analyze a data set for the sake of illustration.

1. Introduction

The failure rate function, also known as the hazard function (HF), is one approach to model life distributions in reliability and survival studies. Typically, researchers assume the hazard function (HF) of interest is either constant or monotonic. However, in practice, HFs may have a non-monotonic behavior, including, but are not limited to, upside-down bathtub-shaped HFs. Such functions increase to a point on the real line and then decrease to become constant later. Langlands et al. (1979) observed this HF in their study, which was about recovering from breast cancer. The study indicated that the highest mortality rate due to this type of cancer appears approximately three years after the disease was diagnosed; afterward, the mortality decreases slowly over a fixed time interval. In literature, three well-known continuous probability distributions have similar upside-down bathtub-shaped HFs: the log-normal distribution, the inverse-normal distribution, and Birnbaum-Saunders (BS) distribution. The HF of the latter model decreases and becomes stable at a positive constant; on the other hand, the HFs of the two former ones tend to zero; see, e.g., Johnson et al. (1995) and Nelson (2009).

Birnbaum and Saunders (1969) introduced the two-parameter BS distribution as a lifetime model for fatigue failure caused due to cyclic loading. The cumulative distribution function (CDF) of the BS distribution is given by

$$F(x; \alpha, \beta) = \Phi\left[\frac{1}{\alpha}\left(\sqrt{\frac{x}{\beta}} - \sqrt{\frac{\beta}{x}}\right)\right], \quad x > 0, \ \alpha, \beta > 0, \quad (1)$$

where $\Phi(\cdot)$ is the standard normal CDF, while α and β are the shape and scale parameters, respectively. Desmond (1985) provided a more general derivation for the BS distribution based on a biological model, and strengthened the physical rationalization for the use of the BS distribution by relaxing the original presumptions of Birnbaum and Saunders (1969). In practice, the scale parameter of the BS distribution represents the median of failure time. Bourguignon et al. (2020) recently proposed control charts for monitoring the median of the BS distribution. Hassani et al. (2020) proposed an extended BS distribution to model *bicoid* gene expression data, while Kannan et al. (2020) designed the repetitive group sampling plan under BS distribution. In the field of multivariate statistics, Saulo et al. (2019) recently discussed inference for the mean-based bivariate BS distributions and corresponding application. Diáz-Garciá and Leiva-Sánchez (2005, 2007) proposed a generalization for the BS distribution which is more flexible than the BS distribution in terms of the kurtosis. The generalized BS (GBS)

* Corresponding author.
  E-mail address: fmalam@kau.edu.sa (F.M.A. Alam).

distribution is based on the idea of replacing the Gaussian kernel in the CDF of the BS distribution with the kernels of elliptically contoured distribution such as the logistic distribution. Balakrishnan et al. (2007) developed sampling plans from truncated life tests assuming the GBS distribution, while Leiva et al. (2008) used the GBS distribution to model air pollutant concentration. For further details in this connection; see Sanhueza et al. (2008). A recent, concise and comprehensive review of various developments on the BS distribution and its generalization can be found in Balakrishnan and Kundu (2019).

Determining the highest point of the hazard rate peak is convenient in practice. Knowing such an instant of change allows researchers to make sound interventions to the phenomenon under study. For instance, suppose that medical researchers have started administering a specific disease treatment. Once they determine when the hazard rate starts to decrease, they can reduce the dosage and, consequently, reduce the treatment cost. In the literature, Kundu et al. (2008) considered estimating the highest point of the peak (i.e., the critical point) of the HF of the well-known BS distribution. They proved that the latter function is unimodal for all shape parameter values (see also Bebbington et al. (2008) in this connection). They also discussed the numerical means to obtain the critical point, conducted some assessments via Monte Carlo simulations, and performed data analysis to illustrate their findings. Azevedo et al. (2012) discussed the critical point of the hazard function in the case of Student's t BS distribution, a particular case of the generalized BS distribution, and a generalization for both the BS distribution and Cauchy BS distribution. They performed a numerical application to evaluate the estimation efficiency of the critical points using different estimation methods and to demonstrate their results.

This paper discusses the form of the HF of the logistic BS (LBS) distribution, which is a particular case of the generalized BS distribution. Determining the highest point of the peak of the hazard rate of the LBS distribution and discussing associated inference have not been considered yet. Furthermore, as previously discussed, this topic is of interest to researchers who perform reliability and survival analyses. Hence, this what makes this study novel. The main objectives of this work are (1) to present a mathematical study of the shape and critical point of the HF of the LBS distribution; (2) to numerically evaluate the critical point estimation efficiency based on moment estimators using Monte Carlo simulations; and (3) to perform a real-life data analysis to compare the findings of this work to previous research.

The rest of this paper is organized as follows. In Section 2, we review the LBS distributions and some of its key properties. In Section 3, we study the shape of the HF of the LBS distribution and the means to estimate its critical value are discussed in Section 4. To evaluate the performance of the proposed estimators of the critical value of the HF, we conduct a Monte Carlo simulation study and its outcomes are reported in Section 5. In Section 6, we analyze a real data set for the sake of illustration. Finally, the paper is concluded in Section 7.

2. LBS distribution

A non-negative continuous random variable X is said to follow the GBS distribution based on an elliptically contoured kernel; say, $G(\cdot)$ with shape parameter $\alpha > 0$, scale parameter $\beta > 0$, and a location parameter γ, if the corresponding CDF is given by:

$$F(x; \alpha, \beta, \gamma) = G\left(\frac{1}{\alpha}\left[\sqrt{\frac{x-\gamma}{\beta}} - \sqrt{\frac{\beta}{x-\gamma}}\right]\right), \quad x > \gamma \geqslant 0, \ \alpha, \beta$$
$$> 0. \tag{2}$$

Now, under the assumption that $\gamma = 0$, if we replace the kernel $G(\cdot)$ in (2) by the CDF of the logistic distribution $G(z) = [1 + \exp(-z)]^{-1}$, then the random variable X is said to follow the BS distribution based on the logistic kernel with shape parameter $\alpha > 0$ and scale parameter $\beta > 0$, i.e., $X \sim \mathrm{LBS}(\alpha, \beta)$. The CDF, probability density function (PDF) and survival function (SF) of the LBS distribution are given by:

$$F(x; \alpha, \beta) = \left\{1 + \exp\left(-\alpha^{-1}\left[\frac{x-\beta}{\sqrt{\beta x}}\right]\right)\right\}^{-1}, \tag{3}$$

$$f(x; \alpha, \beta) = \frac{x^{-\frac{3}{2}}(x+\beta)}{2\alpha\sqrt{\beta}}F(x; \alpha, \beta)S(x; \alpha, \beta), \tag{4}$$

and $S(x; \alpha, \beta) = 1 - F(x; \alpha, \beta)$, respectively. If $X \sim \mathrm{LBS}(\alpha, \beta)$ and $Z \sim \mathrm{Logistic}(0,1)$, then $X = 4^{-1}\beta\left[\alpha Z + \sqrt{4 + \alpha^2 Z^2}\right]^2 \sim \mathrm{LBS}(\alpha, \beta)$ and $Z = \alpha^{-1}(\beta X)^{-\frac{1}{2}}(X - \beta) \sim \mathrm{Logistic}(0,1)$. Based on these relationships, and by using the distributional properties of the standard logistic random variable Z, one can determine the distributional aspects of X. For example, using these relations, one can easily verify that the median is simply equal to β, while $E(X) = \beta(1 + \frac{\pi^2}{6}\alpha^2)$ and $V(X) = \frac{(\alpha\beta\pi)^2}{3}\left(1 + \frac{37}{60}\pi^2\alpha^2\right)$.

3. The HF of the LBS distribution

The HF is a crucial distributional property that has diverse practical applications. For instance, it allows researchers to characterize a probability distribution behavior. Researchers must correctly specify the HF; otherwise, they could encounter severe consequences in the estimation technique due to incorrectly identifying the HF; see Bhatti (2010) in this connection. In practice, the HF can be constant, increasing, decreasing, or non-monotonic. One approach to identifying the HF type is by examining the scaled total test time (TTT) curve proposed by Aarset (1987). This section discusses the HF of the LBS distribution which is given by: $h(x; \alpha, \beta) = f(x; \alpha, \beta)/S(x; \alpha, \beta)$ for $x > 0$ and $0 < S(x; \alpha, \beta) < 1$, where $f(x; \alpha, \beta)$ and $S(x; \alpha, \beta)$ are the PDF and SF of the LBS distribution, respectively. Fig. 1 presents the HF for different values of the shape parameter α, assuming that the scale parameter β is equal to 1,
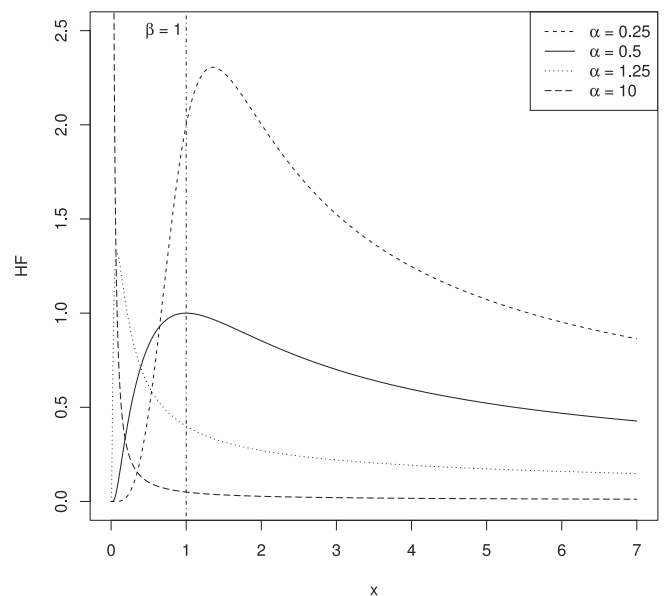

Fig. 1. The HF for the LBS distribution with different values for α and $\beta = 1$.

without loss of generality. The following theorem discusses the shape of the HF of the LBS distribution.

Theorem 1. *If a random variable X follows the LBS distribution with shape parameter $\alpha > 0$ and scale parameter $\beta > 0$, i.e., $X \sim \text{LBS}(\alpha, \beta)$, then the corresponding HF is given by:*

$$
\begin{aligned}
h(x; \alpha, \beta) &= \frac{x^{-\frac{3}{2}(x+\beta)}}{2\alpha\sqrt{\beta}} F(x; \alpha, \beta) \\
&= \frac{x^{-\frac{3}{2}(x+\beta)}}{2\alpha\sqrt{\beta}} \left\{ 1 + \exp\left(-\alpha^{-1}\left[\frac{x-\beta}{\sqrt{\beta x}}\right]\right) \right\}^{-1}.
\end{aligned}
\tag{5}
$$

The curve of the HF $h(x; \alpha, \beta)$ is an upside-down bathtub shaped (i.e., unimodal) curve with a critical point $c_{\alpha,\beta}$ that is obtained by solving the following nonlinear equation

$$
\frac{(x+\beta)^2}{2\alpha\sqrt{\beta}} S(x; \alpha, \beta) - \frac{\sqrt{x}}{2}(x+3\beta) = 0,
$$

such that $c_{\alpha,\beta} \geqslant (<)\beta$ when $\alpha \leqslant (>)0.5$. Nevertheless, if the actual value of the shape parameter is large (i.e., $\alpha \to \infty$), then the HF $h(x; \alpha, \beta)$ is decreasing.

Proof. Observe that the first derivative of the HF (5) with respect to x is given by $h'(x; \alpha, \beta) = 2^{-1}\alpha^{-1}\beta^{-\frac{1}{2}}x^{-3}F(x; \alpha, \beta)g(x; \alpha, \beta)$, such that

$$
g(x; \alpha, \beta) = \frac{(x+\beta)^2}{2\alpha\sqrt{\beta}} S(x; \alpha, \beta) - \frac{\sqrt{x}}{2}(x+3\beta).
\tag{6}
$$

Notice that the sign of $h'(x; \alpha, \beta)$ depends only on the sigh of $g(x; \alpha, \beta)$ which depends on the value of α. Therefore, we need to discuss the cases $\alpha \to \infty$ and $\alpha \nrightarrow \infty$ separately. **Case I:** $\alpha \to \infty$: Clearly, the limit of $g(x; \alpha, \beta)$ as α becomes large is given by:

$$
\lim_{\alpha \to \infty} g(x; \alpha, \beta) = -\frac{\sqrt{x}}{2}(x+3\beta), \ \forall x.
$$

That is, $g(x; \alpha, \beta) < 0$ for all values of x; hence, $h(x; \alpha, \beta)$ is decreasing **Case II:** $\alpha \nrightarrow \infty$: Here, one can observe that as $g(x; \alpha, \beta) > 0$ as $x \to 0$ and $g(x; \alpha, \beta) \to \left(\frac{1}{\alpha} - 2\right)\beta^{\frac{3}{2}}$ as $x \to \beta$. If $c_{\alpha,\beta}$ represents the critical value of $h(x; \alpha, \beta)$, which is the root of expression (6) after equating it to 0, then $c_{\alpha,\beta} \geqslant (<)\beta$ when $\alpha \leqslant (>)0.5$.

4. Critical value estimation

In the previous section, we established that the HF of the LBS distribution has either a unimodal or a decreasing curve. Thus, it is then of natural interest to determine the corresponding critical point $c_{\alpha,\beta}$. Based on Theorem 1, $c_{\alpha,\beta}$ can be obtained as the solution of $g(x; \alpha, \beta)$ which was given by (6). Nevertheless, the solution depends on the model parameters, which need to be estimated first. We propose to estimate them using the modified moments estimation method proposed by Ng et al. (2003), who noticed that the MMEs are easier to use than the maximum likelihood estimators (MLEs) and both share similar behaviors. Let $x_1, \ldots, x_n$ represent an observed random sample of size n from the LBS distribution with PDF as in (4). For the critical value $c_{\alpha,\beta}$, the MME is simply $c_{\tilde{\alpha},\tilde{\beta}} = \tilde{c}$, such that $\tilde{\alpha} = \sqrt{\left(\frac{6}{\pi^2}\left[\sqrt{\left(\frac{s}{r}\right)} - 1\right]\right)}$ and $\tilde{\beta} = \sqrt{sr}$ are the MMEs of α and β, respectively, where $s = n^{-1}\sum_i^n x_i$ and $r^{-1} = n^{-1}\sum_i^n x_i^{-1}$.

Clearly, the MME of $c_{\alpha,\beta}$ does not have an explicit expression; therefore, we seek to obtain a functional approximation of $c_{\alpha,\beta}$ as a function of the model parameters α and β. By following the same approach as in Kundu et al. (2008), we obtain an approximated

MME (AMME) for $c_{\alpha,\beta}$ as follows. Recall that β is a scale parameter; thus, it is obvious that since $c_{\alpha,\beta}$ is the critical point of the HF of the LBS distribution, then $c_{\alpha,\beta} = \beta c_{\alpha,1}$. By using Box-Cox transformation, we observed that $[c_{\alpha,1}]^{-0.5}$ is approximately a linear function of α and so a reasonably good approximation of $\beta c_{\alpha,1}$; say, $c_{\alpha,1}^*$ is given by $c_{\alpha,1}^* = (-0.47633 + 3.22458\alpha)^{-2}$ given that the actual value of α is approximately greater than 0.15. Accordingly, the AMME of $c_{\alpha,\beta}^*$ is simply $c_{\tilde{\alpha},\tilde{\beta}}^* = \tilde{c}^* = \tilde{\beta}(-0.47633 + 3.22458\alpha)^{-2}$.

5. Simulation outcomes

This section reports the outcomes of a Monte Carlo simulation study which have been conducted to numerically examine the estimation efficiency of the proposed estimators mentioned in the preceding section assuming different values for the shape parameter and various sample sizes. The simulation outcomes are reported up to three decimal digits in Table 1 since they are computed based on $M = 10,000$ simulation runs. The latter simulation runs provides an accuracy of the order $\pm(10,000)^{-0.5} = \pm0.01$ (Karian and Dudewicz, 1999). The considered sample sizes were $n = 25, 50, 75, 100, 250, 500$ and $\alpha = 0.5, 1.0$ and 2.0 as the values of the shape parameter. Without loss of any generality, we set the scale parameter $\beta = 1$ for all cases. According to the chosen values of the model parameters, the values of the critical point $c_{\alpha,\beta}$ are obtained by solving expression (6) after equating it to 0. It is to be noted that all computations were performed using an **R** program which is available upon request from the authors.

The MME and AMME are then obtained for $c_{\alpha,\beta}$, and for each estimate, we obtained the bias, the root-mean-squared error (RMSE), the average absolute difference between the true and estimate hazard functions (D_{abs}) and the maximum absolute difference between the true and estimate hazard functions (D_{max}), respectively, as

$$
\text{Bias}(\tilde{c}) = \frac{1}{M}\sum_{i=1}^{M}(\tilde{c}_i - c_{\alpha,\beta}), \quad \text{Bias}(\tilde{c}^*) = \frac{1}{M}\sum_{i=1}^{M}(\tilde{c}_i^* - c_{\alpha,\beta}),
$$

$$
\text{RMSE}(\tilde{c}) = \sqrt{\frac{1}{M}\sum_{i=1}^{M}(\tilde{c}_i - c_{\alpha,\beta})^2}, \quad \text{RMSE}(\tilde{c}^*) = \sqrt{\frac{1}{M}\sum_{i=1}^{M}(\tilde{c}_i^* - c_{\alpha,\beta})^2},
$$

$$
D^{\text{abs}}(\tilde{c}) = D_1^{\text{abs}} = \frac{1}{M}\sum_{i=1}^{M}\left|h(c_{\alpha,\beta}; \alpha, \beta) - h(\tilde{c}_i; \tilde{\alpha}_i, \tilde{\beta}_i)\right|
$$

$$
D^{\text{abs}}(\tilde{c}^*) = D_2^{\text{abs}} = \frac{1}{M}\sum_{i=1}^{M}\left|h(c_{\alpha,\beta}; \alpha, \beta) - h(\tilde{c}_i^*; \tilde{\alpha}_i, \tilde{\beta}_i)\right|
$$

$$
D^{\text{max}}(\tilde{c}) = D_1^{\text{max}} = \max_{i=1,\ldots,M}\left|h(c_{\alpha,\beta}; \alpha, \beta) - h(\tilde{c}_i; \tilde{\alpha}_i, \tilde{\beta}_i)\right|
$$

and

$$
D^{\text{max}}(\tilde{c}^*) = D_2^{\text{max}} = \max_{i=1,\ldots,M}\left|h(c_{\alpha,\beta}; \alpha, \beta) - h(\tilde{c}_i^*; \tilde{\alpha}_i, \tilde{\beta}_i)\right|
$$

such that $\tilde{\alpha}_i, \tilde{\beta}_i$ are the MME of α and β based on simulation run i, while $\tilde{c}_i$ ($\tilde{c}_i^*$) is the MME (AMME) of $c_{\alpha,\beta}$. Table 1 summarizes the simulation study outcomes and reveals that MME and AMME of $c_{\alpha,\beta}$ become more efficient as the sample size increases. Overall, when the shape parameter is small, namely, when $\alpha \leqslant 0.5$, then the AMME is not performing very well; however, it is more accurate when α is large. As the values of both the sample size and the shape parameter increase, the MME and AMME of $c_{\alpha,\beta}$ are quite similar in terms of the considered comparison criteria.

Table 1

Simulated values of bias and RMSEs of c_α alongside the difference measurements between the true and fitted hazard functions evaluated at the actual and estimate critical points, respectively.

α	n	Bias($\bar{c}$)	Bias($\bar{c}^*$)	RMSE($\bar{c}$)	RMSE($\bar{c}^*$)	D_1^{abs}	D_2^{abs}	$D_1^{\max}$	$D_2^{\max}$
0.5	25	0.046	0.115	0.279	0.792	0.229	0.192	3.500	1.373
	50	0.018	−0.084	0.202	0.397	0.150	0.147	1.366	0.930
	75	0.015	−0.134	0.167	0.315	0.119	0.122	0.783	0.623
	100	0.011	−0.155	0.146	0.284	0.103	0.107	0.615	0.555
	250	0.006	−0.196	0.093	0.240	0.065	0.072	0.371	0.370
	500	0.002	−0.212	0.066	0.232	0.045	0.052	0.251	0.245
1	25	0.069	0.036	0.164	0.108	0.261	0.262	2.463	2.463
	50	0.031	0.012	0.086	0.060	0.188	0.189	2.510	2.509
	75	0.020	0.004	0.061	0.045	0.155	0.155	1.265	1.265
	100	0.014	0.000	0.049	0.037	0.135	0.136	0.946	0.945
	250	0.005	−0.006	0.028	0.023	0.087	0.088	0.523	0.522
	500	0.003	−0.007	0.019	0.017	0.062	0.062	0.379	0.378
2	25	0.011	0.011	0.027	0.028	1.050	1.050	11.987	11.986
	50	0.005	0.005	0.014	0.015	0.761	0.761	8.845	8.845
	75	0.003	0.003	0.010	0.010	0.627	0.627	4.976	4.975
	100	0.002	0.003	0.009	0.009	0.551	0.551	4.346	4.346
	250	0.001	0.001	0.005	0.005	0.347	0.347	1.926	1.925
	500	0.000	0.001	0.003	0.004	0.246	0.246	1.591	1.591

Table 2

Lifetimes of Cavia Porcellus induced with different dosages of Mycobacterium Tuberculosis.

12	44	60	70	95	146
15	48	60	72	96	175
22	52	60	73	98	175
24	53	60	75	99	211
24	54	61	76	109	233
32	54	62	76	110	258
32	55	63	81	121	258
33	56	65	83	127	263
34	57	65	84	129	297
38	58	67	85	131	341
38	58	68	87	143	341
43	59	70	91	146	376

Table 4

EDA outcomes based on the lifetimes of Cavia Porcellus.

Source	Q1	Median	Mean	Q3	SD
Sample	54.75	70	99.8194	112.7500	81.1180
BS	46.2221	77.2931	100.2483	129.2505	78.6338
LBS	49.0734	77.4526	99.8199	122.2434	84.6580

6. Application

This section reports the analysis of a real data set considered by Kundu et al. (2008) to compare between the BS distribution and the LBS distribution. The data consists of the lifetimes of Cavia Porcellus (guinea pigs) induced with different dosages of Mycobacterium Tuberculosis. For this data set, 72 observations are listed in Table 2.

We first estimate the model parameters of both the BS and the LBS distributions and both the MMEs and AMMEs of the critical values of the corresponding hazard functions, then we calculate several explanatory data analysis (EDA) measurements based on the considered data set as well as their approximations based on the estimated model parameters. Moreover, we test the fitted models' suitability to the data using Anderson–Darling (AD) and Cramér-von Mises (CvM) goodness-of-fit tests. Finally, we evaluate the fitted hazard rates using the TTT method.

Table 3 summarizes the estimators of the model parameters and the critical values as well as the corresponding goodness-of-fit statistics, while Table 4 shows the outcomes of EDA measurements. By examining these tables, one can observe that the LBS distribution provided EDA measurements close to those of the observed sample compared to the BS distribution. Furthermore, both AD and CVM goodness-of-fit tests indicated that the LBS distribution is much more suitable for the considered data. Fig. 2 shows the histogram of the data compared to the fitted PDFs.

As indicated above, we used the TTT curve method to compare the LBS distribution and the BS distribution in terms of hazard rates. The empirical TTT curve is given by $W_X(u) = H_X^{-1}(u)/H_X^{-1}(1)$, for $u \in (0,1)$, such that $H_X^{-1}(u) = \int_0^{F_X^{-1}(u)}[1 - F_X(y)]dy$, where $F_X^{-1}(\cdot)$ is the quantile function of a lifetime random variable X. Fig. 3 shows the empirical scaled TTT plot based on the analyzed data alongside the fitted TTT curves of BS and LBS distributions. Since the fitted TTT curves are quite similar, we calculated the average and the maximum absolute differences between the empirical TTT curve and their fitted counterparts of the considered models. For the LBS distribution, the mean and maximum differences were 0.033 and 0.07, respectively, compared to 0.039 and 0.09 for the mean and maximum differences in the case of the BS distribution. The previous results support that the claim that the LBS distribution seems to provide a better fit to the Cavia Porcellus data than the BS distribution.

Table 3

Fitted models based on the lifetimes of Cavia Porcellus.

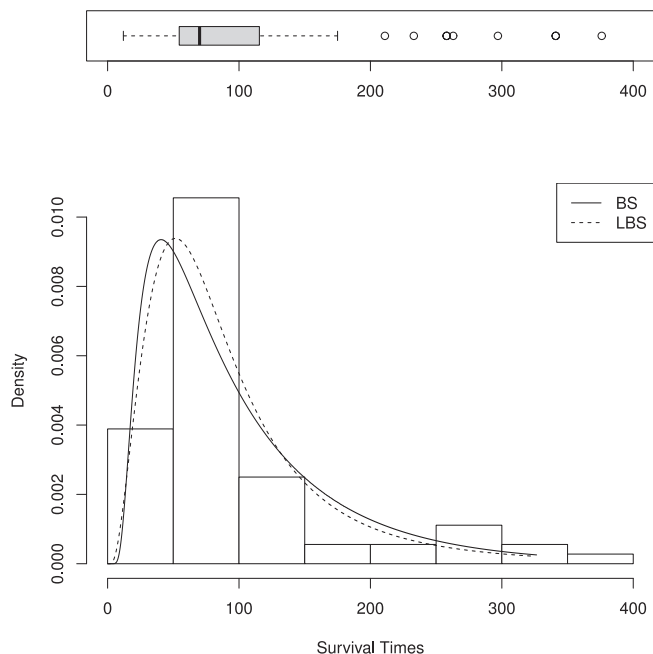| Model	$\tilde{\alpha}$	$\tilde{\beta}$	$\bar{c}$	$\bar{c}^*$	AD	p-value	CVM	p-value
BS	0.7707	77.2931	90.3	87.8	2.0218	0.5327	0.3267	0.6155
LBS	0.4190	77.4526	91.8	101.2	1.9841	0.5503	0.3237	0.6233

Fig. 2. Histogram of the lifetimes of Cavia Porcellus vs. the fitted models.
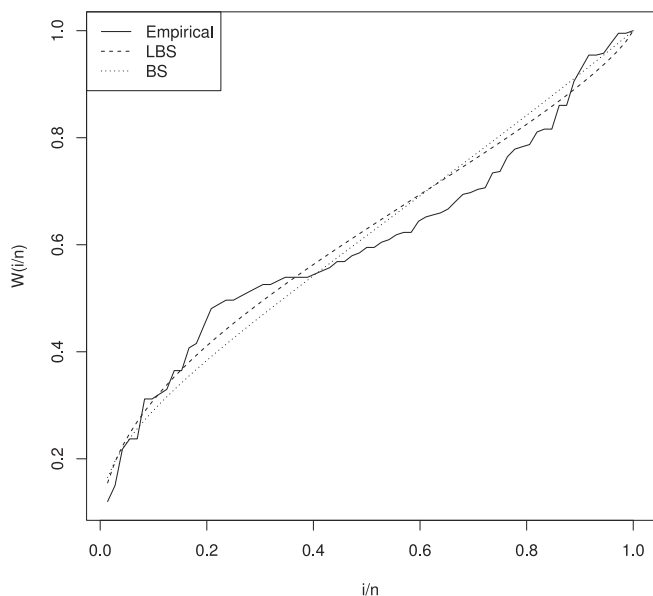

Fig. 3. The fitted TTT curves and the empirical TTT curve based on the lifetimes of Cavia Porcellus..

7. Conclusions

Studying the hazard rate is common in many scientific fields that involve reliability or survival analyses. In statistical literature, researchers might use the BS distribution instead of the lognormal and the inverse Gaussian distributions to model unimodal hazard rates. This study has revealed that the LBS distribution might be more flexible than the BS distribution since the corresponding HF curve can be either decreasing or unimodal. The behavior of the HF mainly depends on the value of the shape parameter *alpha*. The critical point of the hazard function, which represents the highest point of the peak of the hazard rate, has been estimated using two estimators based on the moment estimation methodol-

ogy. Determining the critical point of the HF is vital to researchers since it may reduce any potential costs due to unnecessary interventions to the phenomenon of interest. Based on the Monte Carlo simulation study outcomes, the obtained estimators of the critical points, namely, MME and AMME, performed well as the sample size increases. Both become similar in estimation efficiency for large values of the shape parameter. Therefore, since the AMME of the critical value of the HF has a simple explicit form, we recommend using it given that the actual value of the shape parameter is greater than 0.15. Finally, based on a real data analysis, it is concluded that the LBS distribution might provide a better fit to real-life data compared to the well-known BS distribution. Therefore, The LBS distribution should be considered one of the lifetime distributions used to model either decreasing or unimodal hazard rates.

Several research directions need further investigation in the future. First, one can obtain different point estimators for the critical point of the HF in the case of the LBS distribution. The statistical literature is rich with other frequentist estimation methods (e.g., least-squares methods) and the Bayesian estimation approach. Thus, one may consider conducting a comparative study to examine these methods' performances numerically. Assuming some censoring in the data is another potential research problem that needs to be addressed. A final research area that one might consider is obtaining the asymptotic joint distributions of different estimators and accordingly derive asymptotic confidence intervals compared to bootstrap confidence intervals in terms of lengths and coverage probabilities.

Declaration of Competing Interest

The authors declare that they have no known competing financial interests or personal relationships that could have appeared to influence the work reported in this paper.

Acknowledgments

References

Aarset, M.V., 1987. How to identify a bathtub hazard rate. IEEE Transactions on Reliability R-36, 106–108.

Azevedo, C., Leiva, V., Athayde, E., Balakrishnan, N., 2012. Shape and change point analyses of the Birnbaum–Saunders–t hazard rate and associated estimation. Computational Statistics and Data Analysis 56, 3887–3897.

Balakrishnan, N., Kundu, D., 2019. Birnbaum-saunders distribution: A review of models, analysis, and applications. Applied Stochastic Models in Business and Industry 35, 4–49.

Balakrishnan, N., Leiva, V., López, J., 2007. Acceptance sampling plans from truncated life tests based on the generalized birnbaum–saunders distribution. Communications in Statistics – Simulation and Computation 36, 643–656.

Bebbington, M., Lai, C.D., Zitikis, R., 2008. A proof of the shape of the Birnbaum-Saunders hazard rate function. Mathematical Sciences 33, 49–56.

Bhatti, C.R., 2010. The Birnbaum-Saunders autoregressive conditional duration model. Mathematics and Computers in Simulation 80, 2062–2078.

Birnbaum, Z., Saunders, S., 1969. A new family of life distributions. Journal of Applied Probability 6, 319–327.

Bourguignon, M., Ho, L.L., Fernandes, F.H., 2020. Control charts for monitoring the median parameter of birnbaum-saunders distribution. Quality and Reliability Engineering International 36, 1333–1363.

Desmond, A., 1985. Stochastic models of failure in random environments. Canadian Journal of Statistics 13, 171–183.

Díaz-Garciá, J.A., Leiva-Sánchez, V., 2005. A new family of life distributions based on the elliptically contoured distributions. Journal of Statistical Planning and Inference 128, 445–457.

Díaz-Garciá, J.A., Leiva-Sánchez, V., 2007. Erratum to A new family of life distributions based on the elliptically contoured distributions: [J. Statist.

Plann. Inference, 128 (2), (2005) 445–457]. Journal of Statistical Planning and Inference 137, 1512–1513..

Hassani, H., Kalantari, M., Entezarian, M.R., 2020. A new five-parameter birnbaum–saunders distribution for modeling bicoid gene expression data. Mathematical Biosciences 319, 108275.

Johnson, N.L., Kotz, S., Balakrishnan, N., 1995. Continuous Univariate Distributions, vol. 2. John Wiley & Sons. 2nd Ed..

Kannan, G., Jeyadurga, P., Balamurali, S., 2020. Economic design of repetitive group sampling plan based on truncated life test under birnbaum–saunders distribution. Communications in Statistics – Simulation and Computation, 1–17.

Karian, Z., Dudewicz, E., 1999. Modern Statistical Systems and GPSS Simulations. CRC Press. .

Kundu, D., Kannan, N., Balakrishnan, N., 2008. On the hazard function of Birnbaum-Saunders distribution and associated inference. Computational Statistics & Data Analysis 52, 2692–2702.

Langlands, A.O., Pocock, S.J., Kerr, G.R., Gore, S.M., 1979. Long–term survival of patients with breast cancer: a study of the curability of the disease. BMJ 2, 1247–1251.

Leiva, V., Barros, M., Paula, G.A., Sanhueza, A., 2008. Generalized birnbaum-saunders distributions applied to air pollutant concentration. Environmetrics 19, 235–249.

Nelson, W.B., 2009. Accelerated Testing. John Wiley & Sons.

Ng, H., Kundu, D., Balakrishnan, N., 2003. Modified moment estimation for the two-parameter Birnbaum-Saunders distribution. Computational Statistics and Data Analysis 43, 283–298.

Sanhueza, A., Leiva, V., Balakrishnan, N., 2008. The generalized birnbaum–saunders distribution and its theory, methodology, and application. Communications in Statistics – Theory and Methods 37, 645–670.

Saulo, H., Leão, J., Vila, R., Leiva, V., Tomazella, V., 2019. On mean-based bivariate birnbaum-saunders distributions: Properties, inference and application. Communications in Statistics – Theory and Methods 49, 6032–6056.